Chondroitin-6-sulfate attenuates inflammatory responses in murine macrophages via suppression of NF-κB nuclear translocation.

Guak-Kim Tan and Yasuhiko Tabata*

Department of Biomaterials, Institute for Frontier Medical Sciences, Kyoto University, Kyoto 606-8507, Japan.

* Corresponding author:

Professor Yasuhiko Tabata

Tel: +81 75 751 4121; fax: +81 75 751 4646

E-mail: yasuhiko@frontier.kyoto-u.ac.jp.

Keywords: inflammation, glycosaminoglycans, chondroitin-6-sulfate, macrophages, anti-inflammatory effects, nitric oxide, NF-κB nuclear translocation.

Abstract

Inflammation is a host protective response to noxious stimuli, and excessive production of pro-inflammatory mediators by macrophages (mφ) can lead to numerous pathological conditions. In this study, immunomodulatory effects of immobilized and soluble glycosaminoglycans (GAGs) on mouse bone marrow-derived mφ were compared by measuring nitric oxide (NO). We demonstrate here that all GAGs studied except for heparin were able to modulate interferon-γ/lipopolysaccharide (IFN-γ/LPS)-induced NO release by mφ to varying extents after 24 h of incubation. In particular, the modulatory activities of soluble chondroitin-6-sulfate (C6S), hyaluronic acid and heparan sulfate altered markedly after covalent immobilization. Among them, soluble C6S exhibited the strongest NO inhibitory activity, and the inhibition was dose- and time-dependent. Moreover, C6S significantly reduced pro-inflammatory cytokines interleukin (IL)-6 and tumor necrosis factor (TNF)-α production by IFN-γ/LPS- or LPS-activated mφ. Specifically, the C6S-mediated suppression of mφ pro-inflammatory phenotype was accompanied by an increase in the IL-10 level, suggesting a possible switch towards anti-inflammatory/wound healing M2 state. In addition, the highest magnitude of inhibitory effects was obtained when cells were pre-treated with C6S prior to IFN-γ/LPS or LPS challenge, suggesting an additional role for C6S in protection against microbial infection. Further investigations reveal that the anti-inflammatory effects of C6S on activated mφ may be ascribed at least in part to suppression of NF-κB nuclear translocation.

1. Introduction

Inflammation is a host protective response to noxious stimuli, such as tissue injury, chemical irritants and infection. It is a finely orchestrated process involves (a) release of chemicals by the injured tissue; (b) recruitment of leukocytes that secrete a multitude of pro-inflammatory mediators to remove damaged tissue or pathogens; and (c) resolution of inflammatory responses [1, 2]. Although inflammation set the stage for the subsequent healing process, excessive production of pro-inflammatory mediators can greatly hinder the process, leading to pathological conditions such as psoriasis, septic shock and autoimmune diseases [3, 4].

Macrophages (mφ), a pivotal component of the innate immune system, are considered as the key player of inflammatory responses [2]. *In vitro*, mφ are typically activated to pro-inflammatory phenotype (a.k.a. M1 mφ) by exposure to a priming signal IFN-γ along with microbial entities such as lipopolysaccharide (LPS) [5]. Recognition of LPS by mφ occurs largely via its engagement with Toll-like receptor 4-myeloid differentiation protein–2 (TLR4/MD2) complex found on the cell membrane. This subsequently triggers intracellular signal transduction, eventually leading to the release and translocation of transcription factor NF-κB (p65 and p50) subunits from cytosol to the nucleus where it promotes the synthesis of pro-inflammatory cytokines TNF-α, IL-6, IL-1β and IL-12 etc [5-7]. In the murine system, these cells can also be easily identified by their production of nitric oxide (NO) catalyzed by inducible NO synthase (iNOS) [5, 8].

On the other hand, *in vitro* exposure of mφ to certain cytokines, such as IL-4 and IL-13, resulted in anti-inflammatory/wound healing subsets (a.k.a. M2 mφ) [5, 9, 10]. Such M2 mφ express relatively lower amount of pro-inflammatory mediators, but higher levels of anti-inflammatory mediators, such as cytokine IL-10 and arginase activity [8-10]. Recent data indicates that the activated mφ are still able to switch their functional phenotypes in response to microenvironmental cues rather than exhibit a stable, distinct phenotype [11]. As such, biomolecules that are able to attenuate mφ inflammatory responses and modulate its phenotypic shift toward the M2 state would be of interest for the design of next-generation therapeutic modalities.

GAGs are linear, heterogeneous polysaccharides that ubiquitously expressed on the cell membrane, as ECM components or as soluble molecules in the body [12]. Among the myriad of cellular activities regulated by these molecules, certain GAGs such as heparan sulfate (HS) and hyaluronic acid (HA) have been shown to coordinate leukocyte recruitment and activation, as well as inflammatory mediator production at the inflamed site [13-15]. Because of their diverse biological activities and therapeutic potential, GAGs have been extensively investigated for tissue engineering applications [16-18].

Chondroitin sulfate (CS) is a major member of the GAG family that predominantly found in cartilage, bone, skin and blood vessels [12]. It consist of repeating disaccharide units of D-glucuronic acid (GlcA) and *N*-acetyl-D-galactosamine (GalNAc) that is usually sulfated at either C-4 (chondroitin-4-sulfate, C4S) or C-6 (chondroitin-6-sulfate, C6S) of GalNAc [12, 19]. The immunomodulatory properties of CS are best demonstrated by its therapeutic

benefits in the treatment of osteoarthritis [20, 21]. *In vitro*, CS (mainly C4S and C6S) effectively reduces the generation of pro-inflammatory cytokines, reactive oxygen species and NO by chondrocytes and synovial cells [22, 23]. Accordingly, CS may exert its anti-inflammatory effects by diminishing the expression of p38MAPK phosphorylation and NF-κB activation in these cells. On the other hand, CS from whale cartilage induced the release of NO, but not of pro-inflammatory cytokines (IL-6, IL-1β, IL-12, prostaglandin E_2 and IFN-γ), by resident mouse peritoneal mφ [24].

Conventionally, the biological activities of GAGs were studied with the molecule in solution [24, 25]. GAGs have also been surface-immobilized or used as scaffold materials for tissue engineering [17, 18, 26, 27]. Studies have shown that immobilization can greatly alter the bioactivity of some GAGs. For example, IFN-γ bound to immobilized-GAGs is biologically active while its activity is inhibited by soluble GAGs [28]. C6S, which is normally devoid of anti-coagulant activities, inhibits thrombin generation when coated on glass surfaces [29]. In another study, cross-linked C6S was reported to be a more potent chondrogenic stimulus for human mesenchymal stem cells than soluble C6S [26]. Despite these findings, the effects of GAG immobilization on its immunomodulatory activity are still poorly documented.

Based on these observations, this study was designed to explore the anti-inflammatory properties of GAGs using mouse bone marrow-derived mφ. To achieve this goal, we first compared the inhibitory effects of major GAGs, presented as either immobilized or soluble molecules, on IFN-γ/LPS-induced NO production by mφ. Given the fact that GAGs exist naturally in both these

forms, we hypothesize that mode of GAG presentation may influence their immunomodulatory properties. In the second part of the study, the anti-inflammatory actions of soluble C6S, the most potent of all GAGs tested, were further elucidated by evaluating the dose- and time dependency of the responses along with the production of major pro- and anti-inflammatory cytokines by mφ. In addition, we sought to identify the mechanism responsible for the anti-inflammatory actions of C6S.

2. Materials and Methods

2.1 Reagents and antibodies

GAGs used in this study includes C6S from shark cartilage, C4S from bovine trachea, HS from bovine kidney (all were purchased from Sigma-Aldrich, Japan), HA (200 kDa; DENKA Co. Ltd., Japan) and heparin (Hp) (Fuso Pharmaceutical Industries Ltd., Japan). GAG solutions were prepared freshly in MilliQ water at indicated concentrations and filtered through a 0.02 µm syringe filter (Millipore Corp., Japan). The prepared GAG solutions were endotoxin-free, as verified by the Limulus amoebocyte lysate (LAL) gelation test (Wako Pure Chemical Industries Ltd., Japan). Gelatin with an isoelectric point of 9 (PI9) was kindly provided by Nitta Gelatin Co., Japan. 1-ethyl-3-(3-dimethylaminopropyl) carbodiimide (EDC) and *N*-hydroxysuccinimide (NHS) were purchased from Nacalai Tesque, Japan. Mφ activating agents lipopolysaccharide (LPS; *Escherichia coli* serotype 055:B5) and recombinant murine IFN-γ were obtained from Sigma-Aldrich and Peprotech, respectively. Recombinant macrophage-colony stimulating factor (M-CSF) was from Peprotech. Iscove's Modified

Dulbecco's Medium (IMDM) was purchased from Invitrogen, Japan. Heat-inactivated fetal bovine serum (HI-FBS) was prepared by heating FBS (Hyclone™ Thermo Scientific Inc., Japan) at 56°C for 30 min. Griess-Romijn Nitrite reagent was from Wako Pure Chemicals Ltd. The antibodies used were: mouse monoclonal anti-iNOS/NOS Type II (BD Biosciences), mouse monoclonal anti-β-actin (Sigma-Aldrich), rabbit polyclonal anti-NF-κB p65 (clone Poly6226; BioLegend), horseradish peroxidase (HRP)-conjugated goat anti-mouse IgG (Cell Signaling Technology, Japan) and Alexa Fluor 488-conjugated goat anti-rabbit IgG (Invitrogen). Hoechst 33342 was from Invitrogen. Other reagents used were all of reagent grade and used without further purification.

2.2 Mouse bone marrow-derived mφ culture

Mφ were isolated from 8-week old male Balb/c mice according to a protocol approved by Kyoto University Animal Care Committee. Briefly, bone marrow was flushed from femurs and tibias, washed once in IMDM containing 2% HI-FBS, followed by removal of erythrocytes using BD Pharm Lyse buffer (BD Biosciences). Cells were then centrifuged at 2,300 *g* for 5 min at 4°C, and resuspended in IMDM supplemented with 20% HI-FBS, 50 ng/ml of M-CSF, 2 mM L-glutamine and 1% penicillin/streptomycin. Approximately 5×10^6 cells were plated in 10-cm bacteriological petri dishes and cultured at 37°C in a humidified incubator in 95% air/5% CO_2. The media was changed on day 4 and cells were harvested on day 7. At this stage, > 97% of adherent cells were pure mφ (both F4/80 and CD11b positive) as assessed by FACS analysis. These cells were used in the following experiments.

2.3 Preparation of GAG-immobilized surfaces

Twenty-four well tissue culture plates (Corning Costar, Japan) were pre-coated with 0.1% PI9 gelatin solution for 1 h at RT. For the covalent immobilization of GAGs to the gelatin layer, carboxylic acid groups of GAGs (100 µg/ml in MilliQ water) were pre-activated with a mixture of 2.5 mM EDC and 5 mM NHS for 15 min at RT. To each well was then added 250 µl of the activated GAG solution, and the plates were agitated gently for 2 h at RT followed by three washes with PBS. Using a DMMD assay for GAG quantification [27], it was determined that approximately 50-60% of the added GAGs was successfully immobilized onto the surface, with no further release of immobilized GAGs into the medium after 24 h incubation of the wells in IMDM at 37°C (results not shown).

2.4 M1 mφ cultured with immobilized or soluble GAGs

Mφ were detached by 10 min incubation with cold 5 mM EDTA-PBS followed by repeated pipetting. After centrifugation at 2,300 *g* for 5 min, 6×10^4 cells were plated onto GAG-immobilized surfaces in IMDM with 0.1% bovine serum albumin (BSA; 500 µl/well). After 1 h incubation at 37°C, cells were elicited to pro-inflammatory (M1) phenotype by adding another 500 µl of IMDM with 2% HI-FBS containing activating agents IFN-γ plus LPS (IFN-γ/LPS) to a final concentration of 20 ng/ml and 100 ng/ml, respectively.

To evaluate the modulatory effects of soluble GAGs on M1 mφ, cells were seeded into uncoated 24-well tissue culture plates for 1 h before exposure to

IFN-γ/LPS for an additional 24 h in the presence of GAGs (100 μg/ml). Culture supernatants were then collected, centrifuged at 2,300 *g* for 5 min at 4°C to remove cellular debris, and stored at -30°C until assayed. Cells seeded into standard tissue culture plates (i.e. without any coatings) and stimulated with or without activating agents were served as positive and non-stimulated (NT) controls, respectively.

2.5 Griess assay for NO measurement

Nitrite, a stable metabolite of NO, was measured in the culture supernatants using a Griess assay as described previously [30]. Briefly, 100 μl of culture supernatant was mixed on a 96-well plate with 100 μl of Griess-Romijn Nitrite reagent (100 mg/ml in MilliQ water). After 10 min of incubation at RT, optical density (OD) at 540 nm was measured using a VersaMax™ microplate reader (Molecular Devices). The values were corrected for background levels of "no cell" blank that contains only GAGs. Preliminary studies indicate background interference by C6S and C4S occurs at the concentration ≥ 100 μg/ml, and so some samples were analyzed after diluted to 50 μg/ml that reproducibly exhibits low background levels. The amount of nitrite in the culture supernatant was calculated using $NaNO_2$ as a standard.

2.6 Measurement of cytokine levels by ELISA

IL-6, TNF-α, IL-10 and TGF-β1 levels in culture supernatants were assayed using commercial ELISA kits from R&D Systems followed the manufacturer's instructions.

2.7 Western blot analysis

Expression of iNOS, arginase I and β-actin was quantified by western blot analysis. Briefly, 2.5 × 10^6 cells were seeded on 10-cm bacteriological dishes for 1 h, followed by activation with IFN-γ/LPS or LPS in the absence or presence of C6S. Cells were then dislodged with 5 mM EDTA/PBS, pelleted, resuspended in cold lysis buffer (0.1% Nonidet P-40, 1 mM EDTA, 150 mM NaCl and 50 mM Tris HCl, pH 7.4) with freshly added protease inhibitor (complete protease inhibitor cocktail tablets; Roche) and sonified (2 x 10 sec). The supernatant was collected after centrifugation at 10,000 *g* for 10 min and assayed for protein content by the BCA assay (Pierce, USA). After heat denaturation, aliquots containing 40 µg of protein were resolved on a 10% SDS-PAGE gel at 20 mA constant current. Proteins were transferred to the polyvinylidene difluoride (PVDF) membrane using a BioRad mini trans-blot cell (30 V, 2 h). The membrane was blocked with 2.5% BSA in Tris-buffered saline (TBS; pH 7.5) containing 0.1% Tween 20 (TBST) for 1 hr at RT before overnight incubation at 4°C with mouse monoclonal anti-iNOS/NOS Type II or anti-β-actin antibodies (both were diluted 1:1000 in blocking buffer). After three 5-min washes in TBST, membranes were incubated with HRP-conjugated goat anti-mouse IgG (1:5000 dilution in TBST) for 1 h. Following repeated washing, immunoreactivity was detected by incubating the membranes with SuperSignal West Pico chemiluminescent substrate (Pierce) for 5 min and visualized with LAS-400 image reader (Fujifilm Life Science Co., Japan).

2.8 Arginase activity assay

Cells treated as described in Section 2.7 were lysed with 120 µl of 0.1% Triton-X 100 containing freshly added protease inhibitor for 30 min at 4°C with gentle shaking, sonified (2 × 10 sec) and centrifuged at 10,000 *g* for 10 min. The protein content was determined by the BCA assay. Arginase activity was measured by determining levels of urea production as previously described with slight modification [31]. Briefly, arginase was activated by adding 50 µl 50 mM Tris-HCl (pH 7.5) with 10 mM $MnCl_2$ to 50 µl of the cell lysate, followed by incubation at 56°C for 10 min. Activated lysate was mixed with 100 µl of 0.5 M arginine solution (pH 9.7). After an incubation of 1 h at 37°C the reaction was stopped with 400 µl of acid mixture ($H_3PO_4/H_2SO_4/H_2O$ at a volume ratio of 1:3:7). The urea formed was measured at 540 nm after mixed with 40 µl of α-isonitrosopropiophenone (9% in absolute ethanol) followed by heating at 95°C for 30 min. A standard curve was prepared using urea of known concentrations (0-150 µg/ml). Arginase activity is defined as *p*mol of urea produced per mg protein per min.

2.9 Immunofluorescence staining for NF-κB nuclear translocation

The effect of C6S on nuclear translocation of NF-κB was evaluated by seeding 6×10^4 cells mφ for 1 h in 8-well Lab-Tek™ chamber slides (Thermo Scientific Inc., Japan), followed by activation with IFN-γ/LPS in the absence or presence of C6S (100 µg/ml). At 15 min and 60 min post-treatment, cells were

rinsed twice with PBS, fixed with 4% PFA (15 min, RT) and washed thrice with PBS. Cells were permeabilised with cold acetone for 10 min at -20°C and blocked for 1 h at RT in TBS containing 2% BSA, 2% normal goat serum (NGS) and 0.2% Triton-X 100. Cells were then stained with rabbit anti-p65 NF-κB antibody (1:200 dilution in TBS containing 2% BSA, 2% NGS and 0.05% Triton-X 100) overnight at 4°C. This was followed by incubation with Alexa Fluor 488 goat anti-rabbit IgG (1:200 dilution in TBS containing 2% BSA and 0.05% Triton-X 100). After each staining, unbound antibodies were washed with TBST. To visualize the nuclei, cells were incubated with 1 μg/ml of Hoechst 33342 for 5 min at RT. After rinsed thrice with TBS, the slides were mounted and examined with an Olympus AX80 fluorescence microscope. Negative controls with the omission of primary antibodies were used for background correction. In each experiment, a minimum of six fields (i.e. ≥ 200 cells) were examined and assessed. Nuclear translocation of NF-κB is given as the ratio between the immunopositive nuclei over the total number of nuclei.

2.10 Statistical analysis

Results are presented as mean ± standard deviation (SD) of at least three independent experiments. Statistical comparisons between groups were performed using Student's *t* test or one-way analysis of variance (ANOVA) with Tukey post hoc test, as appropriate. For arginase assay, statistical significance was determined by the non-parametric Wilcoxon signed rank test. A p value <

0.05 was considered statistically significant. All statistical analyses were done using SPSS 17.0 software (SPSS Inc., Chicago, IL).

3. Results

3.1 Effects of immobilized and soluble GAGs on IFN-γ/LPS-induced NO production by mφ

In the first set of experiments, mouse bone marrow-derived mφ were exposed simultaneously to IFN-γ/LPS and GAGs (either immobilized or soluble) for 24 h, before culture supernatants were assayed for nitrite accumulation as an indicator of NO production (Figure 1). As a positive control of M1 mφ activation, cells seeded into uncoated wells and stimulated with IFN-γ/LPS alone exhibited nearly 36-fold increment (7.1 ± 0.9 μM) in NO levels compared to the NT control. Gelatin coating as a precursor layer for the covalent immobilization of GAGs had no significant effect on NO production in these cells (97.5 ± 2.4% of the positive control values; $p>0.05$). As such, all results obtained were normalized arbitrarily to positive control, which was taken as 100%. As shown in Figure 1, the enhancement of M1 mφ NO production was differentially modulated by immobilized GAGs, in which C4S, HA and HS resulted in small, but statistically significant reduction in NO production by M1 mφ ($p<0.05$). Conversely, effects of GAGs on NO production appeared overall more pronounced when presented to activated cells as soluble molecules: (a) HS dramatically increased NO production by M1 mφ up to 151 ± 22% ($p<0.05$); (b) NO levels remained unchanged in the presence of Hp or HA; and (c) both

C6S and C4S reduced NO production to 51 ± 8% and 71 ± 9% (p<0.05), respectively (Figure 1).

As an additional control, we also incubated mφ with individual GAG in the absence of activating agents for 24 h and measured NO levels in culture supernatants. The levels were negligible for all the GAGs, indicating that these molecules alone do not provoke inflammatory responses nor do they contain microbial contaminants (data not shown).

3.2 Dose- and time-dependent suppression of mφ NO production by C6S

We next examined the dose-relationship between C6S, the most efficacious inhibitor determined above, and NO production by M1 mφ. As shown in Figure 2a, soluble C6S exerted a biphasic effect on NO production by cells, in which it suppressed its production in a dose-dependent manner from 10-100 μg/ml, followed by a reversion to control values at higher concentrations. Of note, C6S did not affect mφ viability at the concentrations used, as examined by crystal violet assay (Appendix A). Therefore, any decreases in NO levels could not be attributed to cell death.

On the other hand, no significant changes in NO production were observed in M1 mφ cultured on C6S-immobilzed surfaces with a wide range of coating concentrations (Figure 2b), supporting our hypothesis that the mode of GAG presentation has a great impact on their immunomodulatory properties.

As part of these studies, we also evaluated the effects of C6S on NO production by LPS-activated mφ. As expected, LPS increased the NO release to a lesser extent than IFN-γ/LPS stimulation, resulting in 9-fold increment (1.8 ±

0.5 μM). Likewise, a biphasic response was obtained when these cells were exposed to different C6S concentrations, with maximal inhibition (to 34.4 ± 11% of control levels) also occurring at 100 μg/ml (Figure 2c). This dose was thus used for the subsequent experiments.

The time course of NO production by M1 or LPS-activated mφ in the absence or presence of C6S was also investigated (Figure 3). In positive controls, NO production was readily detected by 4 h post-stimulation and increased in a time-dependent manner. After 24 h, NO production by LPS-activated mφ reached almost the plateau, but in M1 mφ NO release was still increased gradually in a time-dependent manner. In both cases, adding of C6S into the medium attenuated NO production by cells throughout the incubation period. Moreover, C6S caused a 14-h delay in the onset of NO production in LPS-activated mφ (Figure 3b). Nitrite levels in the NT control were negligible throughout the experimental period (data not shown).

3.3 Effects of C6S treatment sequences on NO production

To examine the effects of pre- and post-treatment of C6S on mφ NO production, cells were either pre-treated with C6S for 24 h before an additional 24-h exposure to IFN-γ/LPS or LPS, or *vice versa* (see Appendix B for detailed procedures). As shown in Figure 4, both regimens were effective in reducing NO levels in activated mφ, although different dose-response patterns were obtained. Interestingly, the reduction was more pronounced in the cells that had been pre-treated with C6S, with maximal inhibition (to 33-34% of control levels) was achieved with as low as 50 μg/ml of C6S (Figure 4a). When Figure 2 and

Figure 4 are compared, pre-treatment appears to be the most efficacious regimen among the three treatment sequences (i.e. co-, pre- and post-treatment).

3.4 Effects of C6S on cytokine production by activated mφ

Given the inhibitory effects of C6S on NO production in activated mφ, we asked whether production of major pro-inflammatory (IL-6 and TNF-α) and anti-inflammatory (IL-10 and TGF-β1) cytokines might also be influenced. We first assessed the basal levels of these cytokines in NT and activated mφ (as negative and positive controls, respectively). The NT control constitutively releases low levels of IL-6 and IL-10 (< 12 pg/ml), and relatively higher levels of TNF-α and TGF-β1 (198 ± 15 pg/ml and 282 ± 26 pg/ml, respectively) (Figure 5a). Stimulation of these cells with IFN-γ/LPS or LPS for 24 h elicited robust increases (5-22 folds) in all cytokines except for TGF-β1, with the highest increment was seen in the IL-6 level. Figure 5b shows that the presence of C6S even at low dose (25 μg/ml) was sufficient to reduce IL-6 levels in both activated mφ, with the maximal inhibition was obtained at 100 μg/ml of C6S for M1 mφ. The same dose of C6S also significantly suppressed the production of TNF-α while enhancing the production of IL-10 in activated cells (p<0.05) (Figure 5c). TGF-β1 levels in these cells were unaffected by C6S.

To elucidate the beneficial effects of C6S pre-treatment, we additionally examined the cytokine levels in these samples. Similarly to what we observed in NO production (Figure 4a), C6S pre-treatment exerts greater inhibitory effects

on IL-6 and TNF-α production by activated mφ than co-treatment (Figure 5d). Furthermore, a relatively higher level of IL-10 was noted in M1 mφ that pre-treated with C6S (Figure 5d).

3.5 Effect of C6S on mφ iNOS and arginase expression

To investigate the way in which C6S inhibits NO production, mφ activated for 24 h in the absence or presence of C6S were analyzed for their iNOS level using western blot. As shown in Figure 6a, C6S did not exert significant effects on IFN-γ/LPS-mediated induction of iNOS protein. In LPS-activated cells, however, addition of C6S led to 0.2-0.6 fold decreases in iNOS levels (p<0.05).

We next examined the influence of C6S on mφ arginase, an enzyme that metabolizes the substrate (L-arginine) of iNOS. Compared with the NT control, IFN-γ/LPS significantly reduced mφ arginase activity up to 59%, and this effect was abolished in the presence of C6S (Figure 6b). On the other hand, LPS significantly increased arginase activity in mφ. In these cells, addition of C6S only intermittently (~45% of experiments performed) augmented arginase activity (Figure 6b).

3.6 Effect of C6S on nuclear translocation of NF-κB in mφ

In a final attempt to determine the mechanism of action of C6S, we evaluated its ability to inhibit NF-κB activation. Cells were stimulated for 15 min or 60 min with IFN-γ/LPS in the absence or presence of C6S, and then examined for nuclear translocation of NF-κB using an antibody against p65

subunit. As seen in Figure 7a and 7b, NT controls exhibit low constitutive nuclear translocation of NF-κB (i.e. less than 15% of cells). A rapid and robust activation of NF-κB was seen in 79 ± 10% of cells within 15 min of IFN-γ/LPS stimulation, while after 60 min the value was gradually declined to 54 ± 10% (Figure 7b). Over the duration of stimulation, NF-κB activation was significantly inhibited by 50-60% with the addition of C6S (Figure 7b).

4. Discussions

Successful resolution of inflammation requires the shutting down of pro-inflammatory mediator production by mφ. In the present study, immunomodulatory effects of immobilized and soluble GAGs (C6S, C4S, HA, Hp and HS) on murine mφ were compared by measuring NO. NO is produced primarily by mφ as a cytotoxic effector against pathogens, but can adversely influence the process by causing collateral tissue damage at high doses [32]. We demonstrate here that all GAGs studied except for Hp were able to modulate IFN-γ/LPS-induced NO release by mφ to varying extents, highlighting the importance of microenvironmental cues for mφ functions. In particular, the modulatory activities of soluble C6S, HA and HS altered markedly after immobilization, with the most striking change was seen in HS (Figure 1). In soluble forms HS enhances inflammatory responses in mφ, as shown here and also by others [24, 33, 34]. Conversely, immobilized HS significantly decreased the NO production by activated mφ. These results support our hypothesis that mode of GAG presentation may influence their immunomodulatory properties.

Overall, the modulatory actions of soluble GAGs on mφ are more apparent than the immobilized molecules. One possible explanation to this is consistent with the normal mode of existence of GAGs *in vivo*. Most GAGs exist naturally as covalent complexes with core proteins to form proteoglycans [12]. In this form, the molecules (binding sites) may not accessible to inflammatory cells including mφ. After injury, GAGs are degraded and released as soluble molecules, resulting in structural modifications and the unmasking of their functional binding sites [15, 35, 36]. In such settings soluble GAGs act as a molecular signal that allows rapid recognition of injury by the host defense system. These molecules also actively participate in the ensuing inflammatory process through specific signaling events [14, 15, 36], albeit the mechanisms and cellular consequences of these signals are only partially understood.

GAGs display high degrees of heterogeneity with regards to degree and pattern of sulfation, molecular size and disaccharide composition [12]. The influence of these factors on GAG bioactivity has been studied extensively [37-39]. According to our knowledge, no other investigations have so far reported on the impact of mode of GAG presentation on mφ functions. It is important to point out, though, that the dose of soluble GAGs (100 µg/well) selected in this study does not equivalent to the amount of surface-immobilized GAGs, which is estimated to be 6-8 µg/cm^2 (i.e. 12.5 – 15.0 µg/well) using a DMMB assay (unpublished data). Further investigations on dose response of individual GAGs are thus required to verify their immunomodulatory activities. Although the results presented here are preliminary, we believe the findings provide useful

insights for the design of effective immunomodulatory therapies for inflammation-associated diseases.

The anti-inflammatory activities of CS have been documented in *in vitro* studies with articular cells [23, 25] and in animal models of osteoarthritis [40]. The effects of CS, particularly C6S, on mφ functions are nevertheless less well characterized. Here we show that soluble C6S exhibited the strongest NO inhibitory activity among the GAGs tested, while surface-immobilized C6S exerted no effect (Figure 1 and Figure 2). In the present work, C6S was covalently conjugated onto the surface using carbodiimide chemistry. Given this method involves reactions through side carboxylic acid groups of C6S, it could block site-specific binding and reduces its bioactivity like those observed here. To address this issue, Wang *et al*. [41] developed a biomimetic attachment system that allows GAGs to be tethered via their chain ends. Interestingly, they found that the CS-immobilized surface enhanced NO production by RAW 264.7 murine mφ. This observation, together with our findings, suggests that surface-immobilized CS shows no beneficial effects on the regulation of NO production by activated mφ.

Apart from inhibiting NO production by activated mφ, C6S in solution also significantly reduced pro-inflammatory cytokines IL-6 and TNF-α production by IFN-γ/LPS- or LPS-activated mφ (Figures 5b and 5c). In addition, we observed an opposite effect of C6S on CpG (a TLR9 ligand)-induced IL-6 production (unpublished data). These results appear to be somewhat contrast to an earlier report by Jin *et al*. [42], who showed that C6S suppressed IL-6 secretion induced by CpG, but not by LPS, in mφ-like J774.1 cells. We speculate that the

differential effects of C6S on pro-inflammatory mediator production are dependent on mφ populations, which were shown differ in their cytokine production after LPS stimulation [43]. TNF-α is a pivotal cytokine in the pathogenesis of inflammation, where it can induce the production of other cytokines including IL-6 [44-46]. Antibody blockade of TNF-α is currently FDA-approved for the treatment of Crohn's disease [47] and rheumatoid arthritis [48], and has been successful in alleviating inflammation. On the other hand, IL-6 is an useful biomarker of numerous inflammation-associated diseases including psoriasis [49], osteoarthritis [50, 51], atherosclerosis [52] and diabetes [53] etc. In a broader context, the inhibitory effects of C6S on both TNF-α and IL-6 could have profound implications for the treatments of these diseases.

Specifically, our data indicates that the C6S-mediated suppression of mφ pro-inflammatory phenotype was also possibly accompanied by changes towards anti-inflammatory/wound healing M2 phenotypes, as evidenced by an increase in the IL-10 level (Figures 5c and 5d). One of the known functions of IL-10 is its ability to inhibit the generation of NO and pro-inflammatory mediators, including TNF-α, IL-6 and IL-1 by IFN-γ/LPS- or LPS-activated mφ [54, 55]. Numerous animal studies also indicate that IL-10 plays essential roles in attenuating excessive inflammatory responses and in promoting wound healing [56-58]. Intriguingly, the basal levels of another anti-inflammatory cytokine TGF-β1 were unaffected by both activating agent stimulation and C6S at 24 h post-treatment (Figure 5). As cytokine production by activated mφ is time-dependent

[59], additional studies (e.g. time-course of TGF-β1 induction) are thus required to elucidate this issue.

The anti-inflammatory effects of C6S as shown in the present work was due to its interactions with mφ, rather than a direct binding of C6S with activating agents or pro-inflammatory mediators that impedes their detection in the supernatants. This idea is supported by our results showing that (a) in the absence of C6S, the release of NO from activated mφ reached almost a plateau between 24 and 48 h post-stimulation, and the same trend was seen even in the presence of C6S (Figure 3); (b) in co-treatment, the presence of excess amount of C6S compared to activating agents (i.e. 100 µg/ml versus 20 ng/ml of IFN-γ and 100 ng/ml of LPS) did not completely block their pro-inflammatory effects; and (c) in the case of pre-treatment where C6S was omitted from media for mφ activation, reduction of inflammatory mediator production could still be observed (Figure 4a and Figure 5d). This hypothesis is also in some way supported by the finding that C4S molecules do not form complex with CpG as examined by size-exclusion chromatography [60].

Current knowledge about the mechanisms that regulate NO synthesis in mφ essentially concerns iNOS and arginase [8, 61]. Our investigation indicates that C6S was able to exert some effects on iNOS protein levels and arginase activity in LPS-activated and M1 mφ, respectively (Figure 5), but the magnitude of their changes is insufficient to explain the observed anti-inflammatory actions of C6S. In contrast, nuclear translocation of NF-κB, a key transcriptional regulator in inflammation, was profoundly suppressed by C6S throughout the experimental period (Figure 7), suggesting the possibility that NF-κB pathway is

a mechanism through which C6S inhibits the production of NO, IL-6 and TNF-α. In support of our observation, the inhibitory effects of CS on NF-κB activation have been described by other investigators for chondrocytes [22, 62], synoviocytes [23] and T cells [63]. Nonetheless, the mechanisms by which C6S inhibits NF--κB activation remains unclear and requires further investigation. There are at least two ways in which C6S can act on NF-κB nuclear translocation: (a) a negative signal may be delivered by C6S following an interaction with their specific receptors on mφ; (b) C6S may act as an antagonist, which interferes with the binding of LPS to membrane receptors (e.g. TLR4) on mφ. Consistent with the latter hypothesis, it was demonstrated that C6S was able to interact with the TLR4 receptor complex in LPS-stimulated chondrocytes [62]. Experiments are currently underway to further investigate our hypotheses.

Lastly, to mimic a more clinically relevant scenario, mφ were exposed to C6S at the same time as activating agents in most of our experiments. We additionally examined whether or not C6S was able to inhibit mφ NO and cytokine production if administered at different times relative to activating agent challenge. We found that all three treatment sequences were effective in reducing NO levels in activated mφ, with the highest magnitude of the inhibitory effects was obtained with pre-treatment (Figure 2 and Figure 4a). We thus speculate that, in addition to its anti-inflammatory effects, C6S may also serve as a potential protective agent against microbial (LPS-induced) infection. Moreover, C6S administered after mφ had polarized to M1 phenotypes (i.e. in the case of post-treatment) was still able to manipulate their NO production

(Figure 4b), revealing remarkable plasticity of mφ, as documented previously by Stout *et al*. [64].

5. Conclusion

This study presents the first evidence demonstrating that immobilization of certain GAGs (C6S, HA and HS) alters their immunomodulatory activities, such that they affect IFN-γ/LPS-induced NO production by murine mφ in ways distinct from soluble GAGs. The data presented here provide further evidence to support the anti-inflammatory and protective roles of soluble C6S. In particular, the C6S-mediated suppression of mφ pro-inflammatory phenotype, possibly accompanied by changes towards anti-inflammatory/wound healing M2 state, offers significant potential for the treatment of inflammatory diseases. The effects of C6S on activated mφ may be ascribed at least in part to suppression of NF-κB nuclear translocation. Experiments are underway to further dissect the anti-inflammatory actions of C6S.

Acknowledgements

We would like to thank Dr. Makoto Matsui for his technical help with western blot assay. GKT is supported by the Japan Society for Promotion of Science (JSPS) Postdoctoral Fellowship for Foreign Researchers. This project was financially supported by JSPS Grant-In-Aid for Scientific Research.

References

[1] Medzhitov R. Origin and physiological roles of inflammation. Nature 2008;454:428-35.

[2] Koh TJ, DiPietro LA. Inflammation and wound healing: the role of the macrophage. Expert Rev Mol Med 2011;13:e23.

[3] Glauser MP, Zanetti G, Baumgartner JD, Cohen J. Septic shock: pathogenesis. Lancet 1991;338:732-6.

[4] Ishihara K, Hirano T. IL-6 in autoimmune disease and chronic inflammatory proliferative disease. Cytokine Growth Factor Rev 2002;13:357-68.

[5] Mantovani A, Sica A, Sozzani S, Allavena P, Vecchi A, Locati M. The chemokine system in diverse forms of macrophage activation and polarization. Trends Immunol 2004;25:677-86.

[6] Chow JC, Young DW, Golenbock DT, Christ WJ, Gusovsky F. Toll-like receptor-4 mediates lipopolysaccharide-induced signal transduction. J Biol Chem 1999;274:10689-92.

[7] Biswas SK, Lewis CE. NF-kappaB as a central regulator of macrophage function in tumors. J Leukoc Biol 2010;88:877-84.

[8] Modolell M, Corraliza IM, Link F, Soler G, Eichmann K. Reciprocal regulation of the nitric oxide synthase/arginase balance in mouse bone marrow-derived macrophages by TH1 and TH2 cytokines. Eur J Immunol 1995;25:1101-4.

[9] Stein M, Keshav S, Harris N, Gordon S. Interleukin 4 potently enhances murine macrophage mannose receptor activity: a marker of alternative immunologic macrophage activation. J Exp Med 1992;176:287-92.

[10] Gordon S, Martinez FO. Alternative activation of macrophages: mechanism and functions. Immunity 2010;32:593-604.

[11] Porcheray F, Viaud S, Rimaniol AC, Leone C, Samah B, Dereuddre-Bosquet N, *et al*. Macrophage activation switching: an asset for the resolution of inflammation. Clin Exp Immunol 2005;142:481-9.

[12] Esko JD KK, Lindahl U. Proteoglycans and sulfated glycosaminoglycans. New York: Cold Spring Harbor Laboratory Press; 2009.

[13] Marshall LJ, Ramdin LS, Brooks T, PC DP, Shute JK. Plasminogen activator inhibitor-1 supports IL-8-mediated neutrophil transendothelial migration by inhibition of the constitutive shedding of endothelial IL-8/heparan sulfate/syndecan-1 complexes. J Immunol 2003;171:2057-65.

[14] Termeer C, Benedix F, Sleeman J, Fieber C, Voith U, Ahrens T, *et al*. Oligosaccharides of hyaluronan activate dendritic cells via toll-like receptor 4. J Exp Med 2002;195:99-111.

[15] Jiang D, Liang J, Fan J, Yu S, Chen S, Luo Y, *et al*. Regulation of lung injury and repair by Toll-like receptors and hyaluronan. Nat Med 2005;11:1173-9.

[16] Flanagan TC, Wilkins B, Black A, Jockenhoevel S, Smith TJ, Pandit AS. A collagen-glycosaminoglycan co-culture model for heart valve tissue engineering applications. Biomaterials 2006;27:2233-46.

[17] Zhong S, Teo WE, Zhu X, Beuerman R, Ramakrishna S, Yung LY. Formation of collagen-glycosaminoglycan blended nanofibrous scaffolds and their biological properties. Biomacromolecules 2005;6:2998-3004.

[18] van Susante JLC, Pieper J, Buma P, van Kuppevelt TH, van Beuningen H, van Der Kraan PM, *et al*. Linkage of chondroitin-sulfate to type I collagen scaffolds stimulates the bioactivity of seeded chondrocytes in vitro. Biomaterials 2001;22:2359-69.

[19] Taylor KR, Gallo RL. Glycosaminoglycans and their proteoglycans: host-associated molecular patterns for initiation and modulation of inflammation. FASEB J 2006;20:9-22.

[20] Kahan A, Uebelhart D, De Vathaire F, Delmas PD, Reginster JY. Long-term effects of chondroitins 4 and 6 sulfate on knee osteoarthritis: the study on osteoarthritis progression prevention, a two-year, randomized, double-blind, placebo-controlled trial. Arthritis Rheum 2009;60:524-33.

[21] Michel BA, Stucki G, Frey D, De Vathaire F, Vignon E, Bruehlmann P, *et al*. Chondroitins 4 and 6 sulfate in osteoarthritis of the knee: a randomized, controlled trial. Arthritis Rheum 2005;52:779-86.

[22] Jomphe C, Gabriac M, Hale TM, Heroux L, Trudeau LE, Deblois D, *et al*. Chondroitin sulfate inhibits the nuclear translocation of nuclear factor-kappaB in interleukin-1beta-stimulated chondrocytes. Basic Clin Pharmacol Toxicol 2008;102:59-65.

[23] Alvarez-Soria ML, Santilana J, Calvo E, Egido J, Herrero-Beaumont G. Differential anticatabolic profile of glucosamine sulfate versus other anti-osteoarthritic drugs on human osteoarthritic chondrocytes and synovial fibroblast in culture (Abstract). Osteoarthritis and cartilage 2005;13:S153.

[24] Wrenshall LE, Stevens RB, Cerra FB, Platt JL. Modulation of macrophage and B cell function by glycosaminoglycans. J Leukoc Biol 1999;66:391-400.

[25] Bassleer CT, Combal JP, Bougaret S, Malaise M. Effects of chondroitin sulfate and interleukin-1 beta on human articular chondrocytes cultivated in clusters. Osteoarthritis Cartilage 1998;6:196-204.

[26] Chen WC, Yao CL, Chu IM, Wei YH. Compare the effects of chondrogenesis by culture of human mesenchymal stem cells with various type of the chondroitin sulfate C. J Biosci Bioeng 2011;111:226-31.

[27] Tan GK, Dinnes DL, Butler LN, Cooper-White JJ. Interactions between meniscal cells and a self assembled biomimetic surface composed of hyaluronic acid, chitosan and meniscal extracellular matrix molecules. Biomaterials 2010;31:6104-18.

[28] Fernandez-Botran R, Yan J, Justus DE. Binding of interferon gamma by glycosaminoglycans: a strategy for localization and/or inhibition of its activity. Cytokine 1999;11:313-25.

[29] Keuren JF, Wielders SJ, Willems GM, Morra M, Cahalan L, Cahalan P, *et al*. Thrombogenicity of polysaccharide-coated surfaces. Biomaterials 2003;24:1917-24.

[30] Ando I, Tsukumo Y, Wakabayashi T, Akashi S, Miyake K, Kataoka T, *et al*. Safflower polysaccharides activate the transcription factor NF-kappa B via Toll-like receptor 4 and induce cytokine production by macrophages. Int Immunopharmacol 2002;2:1155-62.

[31] Corraliza IM, Campo ML, Soler G, Modolell M. Determination of arginase activity in macrophages: a micromethod. J Immunol Methods 1994;174:231-5.

[32] Kolb H, Kolb-Bachofen V. Nitric oxide in autoimmune disease: cytotoxic or regulatory mediator? Immunol Today 1998;19:556-61.

[33] Wrenshall LE, Carlson A, Cerra FB, Platt JL. Modulation of cytolytic T cell responses by heparan sulfate. Transplantation 1994;57:1087-94.

[34] Bussini S, Meda L, Scarpini E, Clementi E, Conti G, Tiriticco M, *et al*. Heparan sulfate proteoglycan induces the production of NO and TNF-alpha by murine microglia. Immun Ageing 2005;2:11.

[35] Kato M, Wang H, Kainulainen V, Fitzgerald ML, Ledbetter S, Ornitz DM, *et al*. Physiological degradation converts the soluble syndecan-1 ectodomain from an inhibitor to a potent activator of FGF-2. Nat Med 1998;4:691-7.

[36] Noble PW. Hyaluronan and its catabolic products in tissue injury and repair. Matrix Biol 2002;21:25-9.

[37] Holmer E, Kurachi K, Soderstrom G. The molecular-weight dependence of the rate-enhancing effect of heparin on the inhibition of thrombin, factor Xa, factor IXa, factor XIa, factor XIIa and kallikrein by antithrombin. Biochem J 1981;193:395-400.

[38] Ogamo A, Nagai A, Nagasawa K. Binding of heparin fractions and other polysulfated polysaccharides to plasma fibronectin: effects of molecular size and degree of sulfation of polysaccharides. Biochim Biophys Acta 1985;841:30-41.

[39] Nikitovic D, Zafiropoulos A, Tzanakakis GN, Karamanos NK, Tsatsakis AM. Effects of glycosaminoglycans on cell proliferation of normal osteoblasts and human osteosarcoma cells depend on their type and fine chemical compositions. Anticancer Res 2005;25:2851-6.

[40] Campo GM, Avenoso A, Campo S, D'Ascola A, Traina P, Calatroni A. Chondroitin-4-sulphate inhibits NF-kB translocation and caspase activation in collagen-induced arthritis in mice. Osteoarthritis Cartilage 2008;16:1474-83.

[41] Wang K, Luo Y. Defined surface immobilization of glycosaminoglycan molecules for probing and modulation of cell-material interactions. Biomacromolecules 2013;14:2373-82.

[42] Jin M, Iwamoto T, Yamada K, Satsu H, Totsuka M, Shimizu M. Effects of chondroitin sulfate and its oligosaccharides on toll-like receptor-mediated IL-6 secretion by macrophage-like J774.1 cells. Biosci Biotechnol Biochem 2011;75:1283-9.

[43] Means TK, Pavlovich RP, Roca D, Vermeulen MW, Fenton MJ. Activation of TNF-alpha transcription utilizes distinct MAP kinase pathways in different macrophage populations. J Leukoc Biol 2000;67:885-93.

[44] Neta R, Sayers TJ, Oppenheim JJ. Relationship of TNF to interleukins. Immunol Ser 1992;56:499-566.

[45] Matsuno H, Yudoh K, Katayama R, Nakazawa F, Uzuki M, Sawai T, *et al*. The role of TNF-alpha in the pathogenesis of inflammation and joint destruction in rheumatoid arthritis (RA): a study using a human RA/SCID mouse chimera. Rheumatology (Oxford) 2002;41:329-37.

[46] Vassalli P. The pathophysiology of tumor necrosis factor. Annual Review of Immunology 1992;10:411-52.

[47] Rudolph SJ, Weinberg DI, McCabe RP. Long-term durability of Crohn's disease treatment with infliximab. Dig Dis Sci 2008;53:1033-41.

[48] Maini MFaRN. Anti-TNF-alpha therapy of rheumatoid arthritis: What have we learned? Annual Review of Immunology 2001;19:163-96.

[49] Fitzgerald O, Chandran V. Update on biomarkers in psoriatic arthritis: a report from the GRAPPA 2010 annual meeting. J Rheumatol 2012;39:427-30.

[50] Kaneko S, Satoh T, Chiba J, Ju C, Inoue K, Kagawa J. Interleukin-6 and interleukin-8 levels in serum and synovial fluid of patients with osteoarthritis. Cytokines Cell Mol Ther 2000;6:71-9.

[51] Richette P, Poitou C, Garnero P, Vicaut E, Bouillot JL, Lacorte JM, *et al*. Benefits of massive weight loss on symptoms, systemic inflammation and cartilage turnover in obese patients with knee osteoarthritis. Ann Rheum Dis 2011;70:139-44.

[52] Larsson PT, Hallerstam S, Rosfors S, Wallen NH. Circulating markers of inflammation are related to carotid artery atherosclerosis. Int Angiol 2005;24:43-51.

[53] Pradhan AD, Manson JE, Rifai N, Buring JE, Ridker PM. C-reactive protein, interleukin 6, and risk of developing type 2 diabetes mellitus. JAMA 2001;286:327-34.

[54] Fiorentino DF, Zlotnik A, Mosmann TR, Howard M, O'Garra A. IL-10 inhibits cytokine production by activated macrophages. J Immunol 1991;147:3815-22.

[55] de Waal Malefyt R, Abrams J, Bennett B, Figdor CG, de Vries JE. Interleukin 10 (IL-10) inhibits cytokine synthesis by human monocytes: an autoregulatory role of IL-10 produced by monocytes. J Exp Med 1991;174:1209-20.

[56] Chmiel JF, Konstan MW, Knesebeck JE, Hilliard JB, Bonfield TL, Dawson DV, *et al*. IL-10 attenuates excessive inflammation in chronic Pseudomonas infection in mice. Am J Respir Crit Care Med 1999;160:2040-7.

[57] Liechty KW, Kim HB, Adzick NS, Crombleholme TM. Fetal wound repair results in scar formation in interleukin-10-deficient mice in a syngeneic murine model of scarless fetal wound repair. J Pediatr Surg 2000;35:866-72; discussion 72-3.

[58] Saadane A, Soltys J, Berger M. Role of IL-10 deficiency in excessive nuclear factor-kappaB activation and lung inflammation in cystic fibrosis transmembrane conductance regulator knockout mice. J Allergy Clin Immunol 2005;115:405-11.

[59] El Gazzar M. HMGB1 modulates inflammatory responses in LPS-activated macrophages. Inflamm Res 2007;56:162-7.

[60] Jin M, Iwamoto T, Yamada K, Satsu H, Totsuka M, Shimizu M. Disaccharide derived from chondroitin sulfate A suppressed CpG-induced IL-6 secretion in macrophage-like J774.1 cells. Cytokine 2010;51:53-9.

[61] Mori M, Gotoh T. Regulation of nitric oxide production by arginine metabolic enzymes. Biochem Biophys Res Commun 2000;275:715-9.

[62] Campo GM, Avenoso A, Campo S, Traina P, D'Ascola A, Calatroni A. Glycosaminoglycans reduced inflammatory response by modulating toll-like receptor-4 in LPS-stimulated chondrocytes. Arch Biochem Biophys 2009;491:7-15.

[63] Rolls A, Cahalon L, Bakalash S, Avidan H, Lider O, Schwartz M. A sulfated disaccharide derived from chondroitin sulfate proteoglycan protects against inflammation-associated neurodegeneration. FASEB J 2006;20:547-9.

[64] Stout RD, Jiang C, Matta B, Tietzel I, Watkins SK, Suttles J. Macrophages sequentially change their functional phenotype in response to changes in microenvironmental influences. J Immunol 2005;175:342-9.

Figure captions

Figure 1. Effects of mode of GAG presentation on IFN-γ/LPS-induced NO production by mφ. Mouse bone marrow-derived mφ were stimulated with IFN-γ/LPS in the presence of either immobilized or soluble GAGs for 24 h, before culture supernatants were assayed for nitrite accumulation as an indicator of NO production (see Materials and Methods for details). Results were normalized and presented as percentage of positive control. † $p<0.05$ versus positive control; * $p<0.05$; n = 3-5 from three independent experiments.

Figure 2. Effects of C6S concentration on NO production by activated mφ. Mφ were stimulated with IFN-γ/LPS for 24 h (a) in the presence of varying concentrations of soluble C6S, or (b) after plated on the C6S-immobilized surfaces (note: the x-axis represents the concentration of C6S coating solution). (c) NO production by LPS-activated mφ in relation to soluble C6S concentration. Nitrite levels in supernatants were measured using a Griess assay as detailed in Materials and Methods. * $p<0.05$; † $p<0.05$ versus all other groups; § $p<0.05$ versus all other groups except 100 μg/ml; # $p<0.05$ versus all other groups except 50 μg/ml; n = 6 from three independent experiments.

Figure 3. Kinetics of NO production by activated mφ in the absence or presence of C6S. Cells seeded into uncoated 24-well tissue culture plates were activated with (a) IFN-γ/LPS (M1) or (b) LPS in the absence (■,▲) or presence (□,△) of 100 μg/ml C6S for 48 h to analysis the accumulation of nitrite in culture supernatants at various time intervals. Shown here are representative plots from three independent experiments performed in duplicate.

Figure 4. Effects of C6S treatment sequences on NO production by activated mφ. IFN-γ/LPS (M1)- or LPS-activated mφ were (a) pre-treated or (b) post-treated for 24 h with the indicated concentrations of C6S as detailed in Appendix B, after which NO levels in culture supernatants were measured. * $p<0.05$ versus 0 μg/ml; n = 9 from three independent experiments.

Figure 5. Cytokine production by mouse bone marrow-derived mφ. (a) Cytokine levels in the NT control and mφ activated with IFN-γ/LPS (M1) or LPS alone for 24 h. (b) Dose-response effects of C6S on IL-6 production by activated mφ. Cells were stimulated with IFN-γ/LPS (M1) or LPS in the presence of varying C6S concentrations for 24 h, after which the supernatants were subjected to ELISA for IL-6. Changes of other cytokine secretion by activated mφ in response to (c) co-treatment or (d) pre-treatment of 100 μg/ml of C6S. †$p<0.05$ versus NT control; * $p<0.05$ versus corresponding control; ** $p<0.01$ versus corresponding control; n = 3-4 from three independent experiments.

Figure 6. Effects of C6S on iNOS and arginase activity in activated mφ. Mφ were stimulated for 24 h with IFN-γ/LPS (M1) or LPS in the absence or presence of 100 μg/ml of C6S. Total cell lysates were then subjected to (a) western blot and density analysis for iNOS expression with β-actin serves as a loading control (n=4), or (b) arginase activity assay (n=6), as described in Materials and Methods. Dotted line indicates arginase activity in NT controls that was set at 100%. Horizontal bars denote medians. * $p < 0.05$; § $p < 0.05$ (Wilcoxon signed rank test).

Figure 7. Effects of C6S on NF-κB nuclear translocation in activated mφ. (a) Representative immunofluorescence images showing nuclear localization of NF-κB p65 (green) in mφ at 15 min after IFN-γ/LPS (M1) stimulation in the absence or presence of C6S. Hoechst 33342 (blue) was used as a nuclear counterstain. Non-stimulated cells (NT) serve as experimental controls. No nuclear NF-κB p65 staining was noted in the negative control with the primary antibody omitted (results not shown). (b) Quantitative analysis was performed by counting the percentage of cells with immunopositive nuclei. † $p<0.05$ versus NT control; * $p<0.05$; n = 4.

Appendices

Appendix A: Assessment of mφ viability using the crystal violet assay

Mouse bone marrow-derived mφ were seeded onto uncoated 24-well tissue culture plates at 6×10^4 cells/well in IMDM with 0.1% BSA. After 1 h at 37°C, cells were incubated with 0-500 µg/ml of C6S for additional 24 h, after which the cells were washed twice with PBS, fixed with 4% PFA (15 min, RT) and stained with 0.1% crystal violet solution in 200 mM MES buffer (pH 6) for 15 min. After washing twice with PBS, 220 µl of 10% glacial acetic acid solution was added to each well to extract the dye. OD at 590 nm was then determined using a VersaMax™ microplate reader (Molecular Devices). The results indicated that C6S has no significant effects on mφ viability at the concentrations used (p>0.05; ANOVA test). Similar findings, not reported here, were obtained in the IFN-γ/LPS (M1)- or LPS-activated mφ.

Appendix B: Scheme for C6S pre- and post-treatments

Mouse bone marrow-derived mφ were seeded onto uncoated 24-well tissue culture plates at 6×10^4 cells/well in IMDM with 0.1% BSA, and incubated for 1 h at 37°C. C6S (100 µg/ml in IMDM with 0.1% HI-FBS) was then added at different times relative to activating agent (i.e. IFN-γ/LPS or LPS) challenges as outlined above. Accumulation of nitrite in culture supernatants, an indicator of NO production by cells, was measured using the Griess assay as described in Section 2.5.

Figure 1.

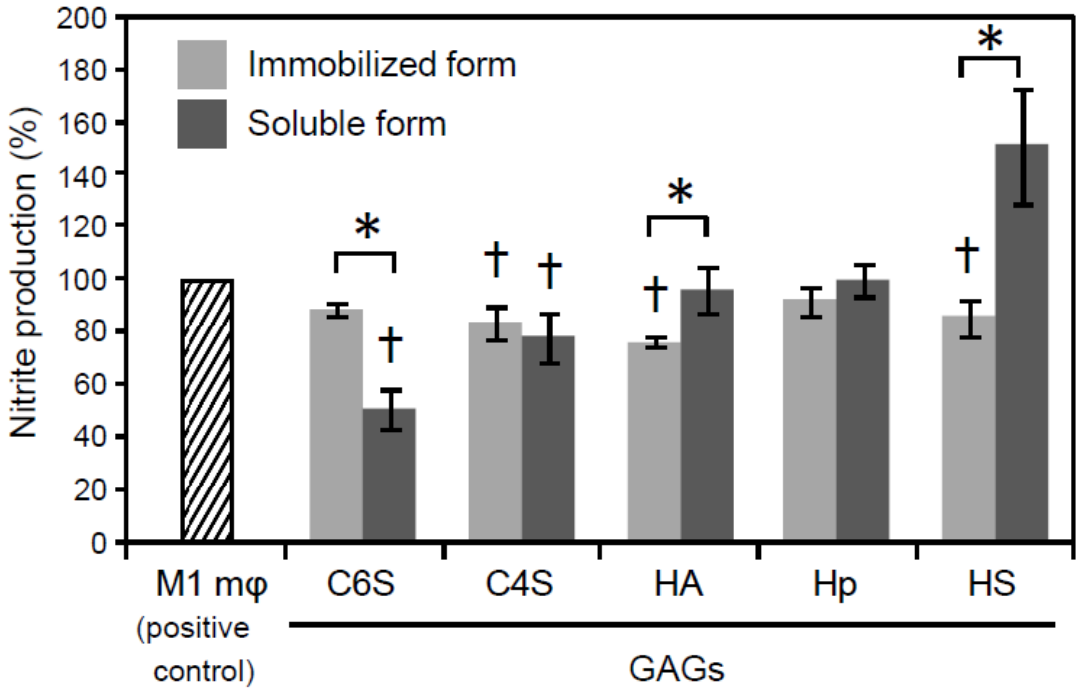
Nitrite production (%)
200
180
160
140
120
100
80
60
40
20
0
Immobilized form
Soluble form
*
*
*
†
†
†
†
†
M1 mφ
(positive
control)
C6S
C4S
HA
Hp
HS
GAGs

Figure 2.

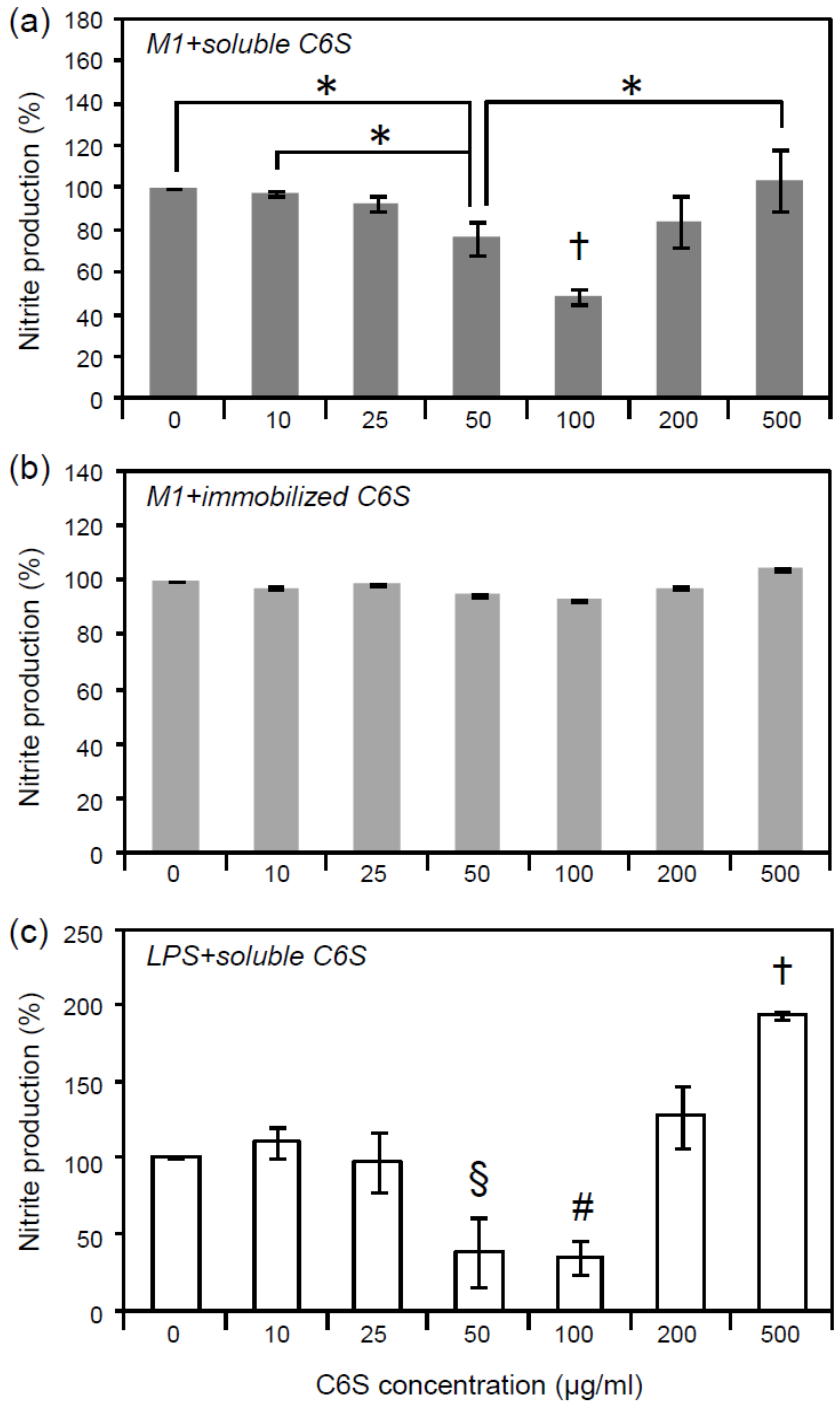
(a)
M1+soluble C6S
Nitrite production (%)
180
160
140
120
100
80
60
40
20
0
*
*
*
†
0
10
25
50
100
200
500
(b)
M1+immobilized C6S
Nitrite production (%)
140
120
100
80
60
40
20
0
0
10
25
50
100
200
500
(c)
LPS+soluble C6S
Nitrite production (%)
250
200
150
100
50
0
§
#
†
0
10
25
50
100
200
500
C6S concentration (μg/ml)

Figure 3.

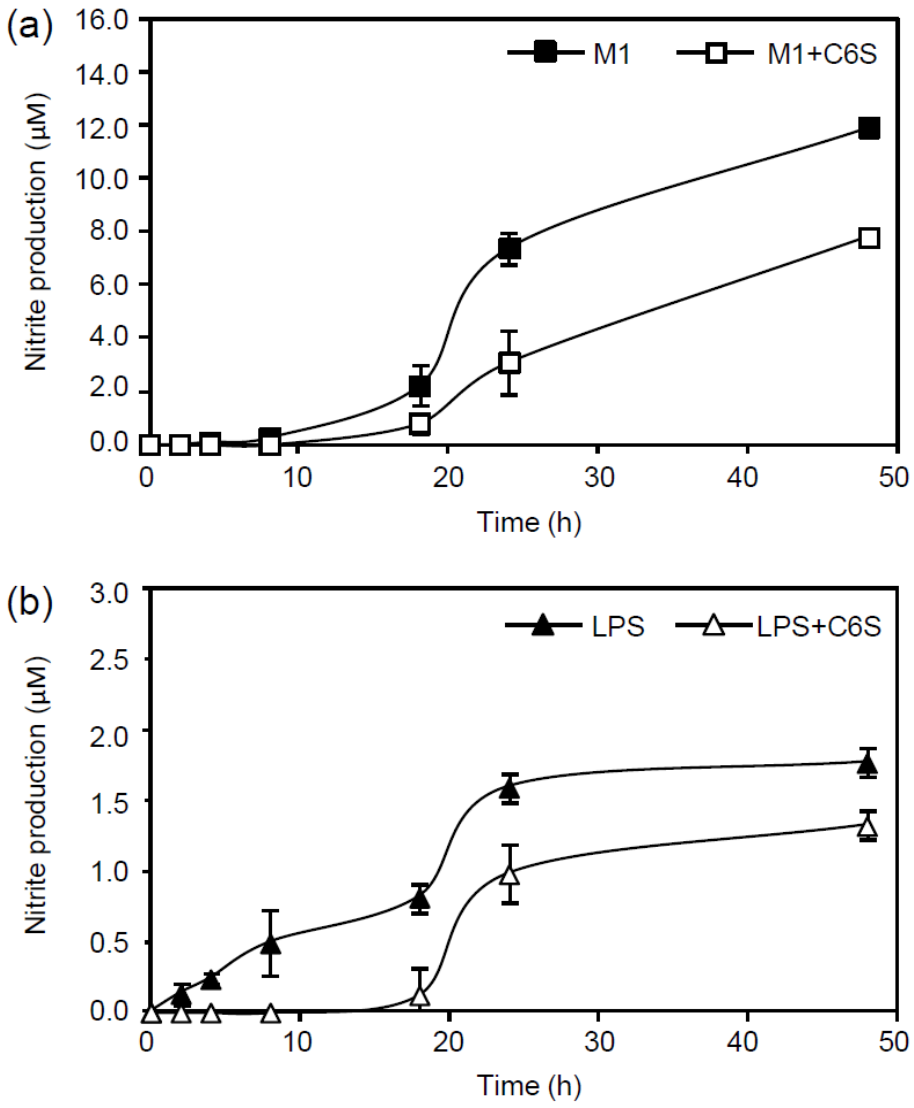
(a)
Nitrite production (μM)
16.0
14.0
12.0
10.0
8.0
6.0
4.0
2.0
0.0
0
10
20
30
40
50
Time (h)
M1
M1+C6S
(b)
Nitrite production (μM)
3.0
2.5
2.0
1.5
1.0
0.5
0.0
0
10
20
30
40
50
Time (h)
LPS
LPS+C6S

Figure 4.

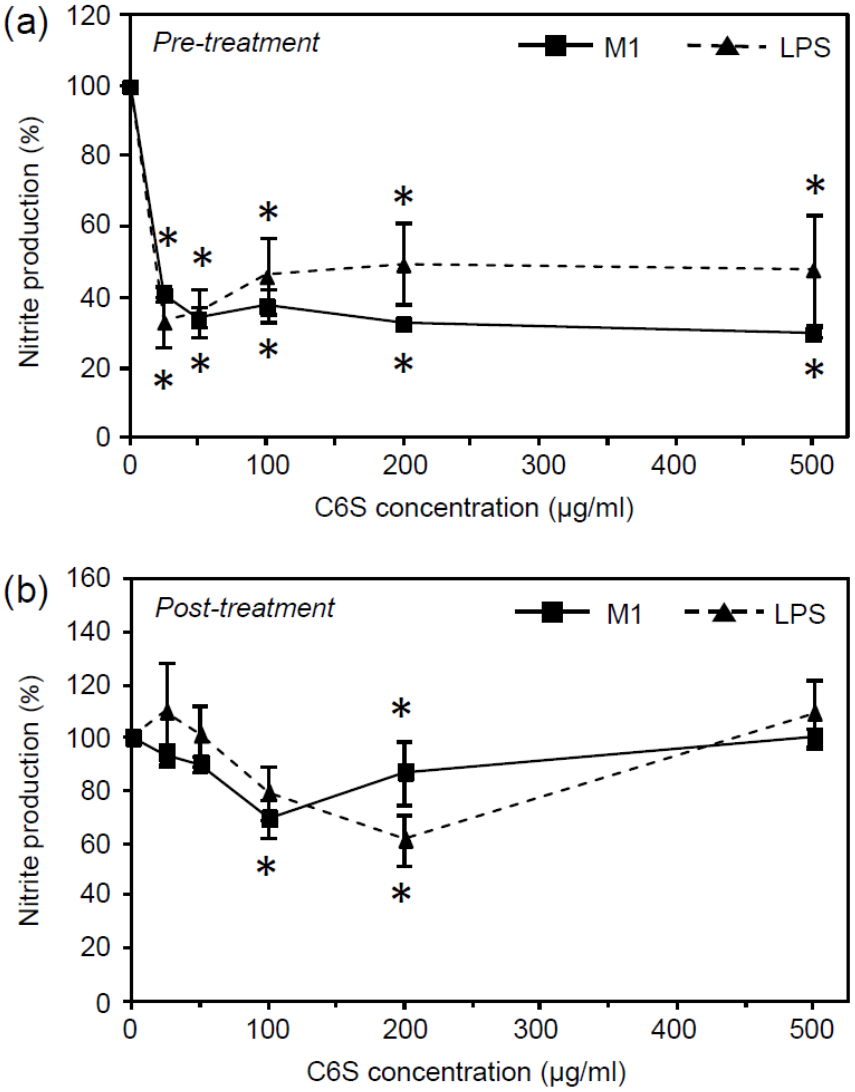
(a)
Pre-treatment
M1
LPS
Nitrite production (%)
C6S concentration (μg/ml)
(b)
Post-treatment
M1
LPS
Nitrite production (%)
C6S concentration (μg/ml)

Figure 5.

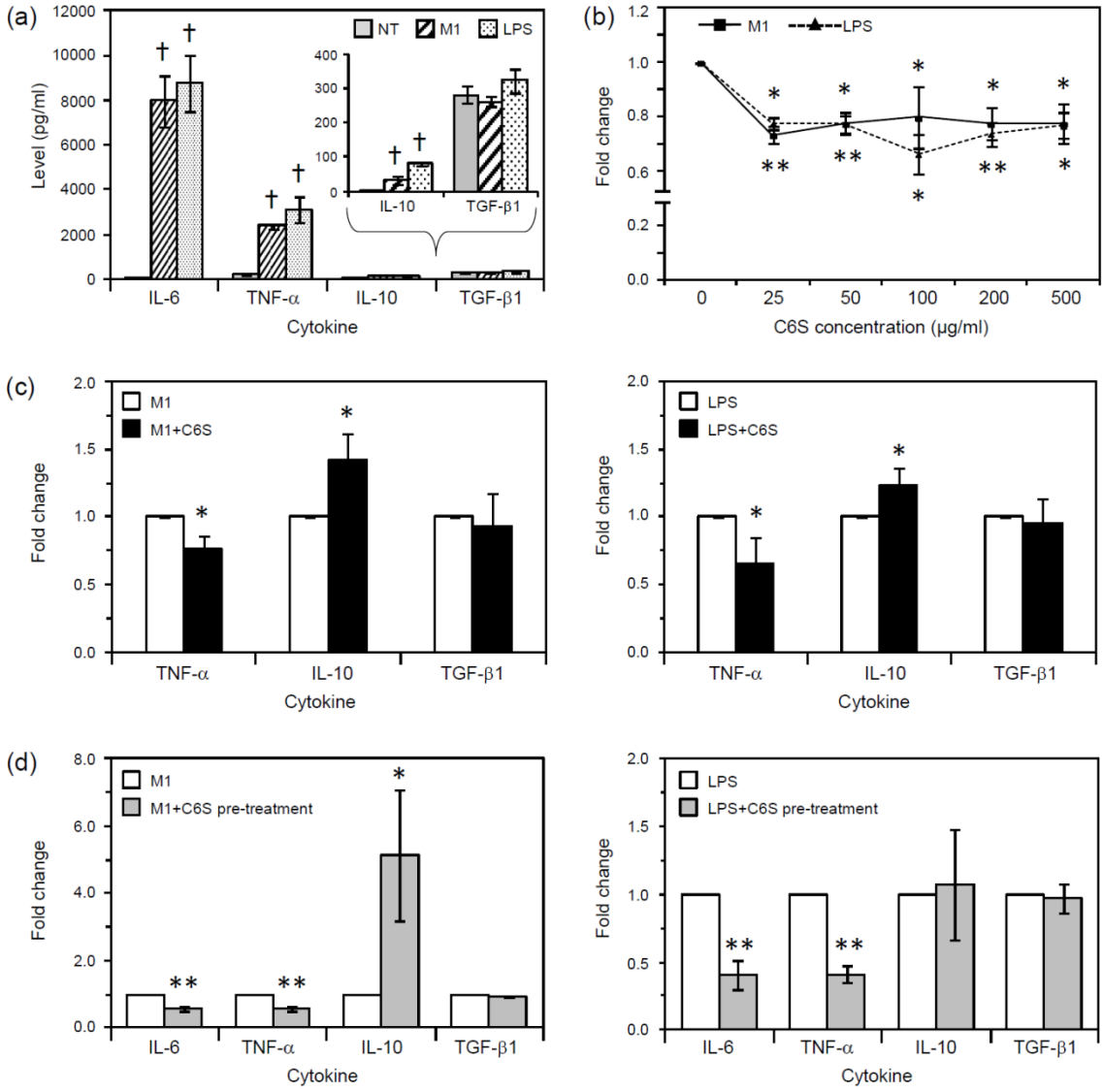
(a)
NT
M1
LPS
Level (pg/ml)
IL-6
TNF-α
IL-10
TGF-β1
Cytokine
(b)
M1
LPS
Fold change
C6S concentration (μg/ml)
(c)
M1
M1+C6S
LPS
LPS+C6S
Fold change
TNF-α
IL-10
TGF-β1
Cytokine
(d)
M1
M1+C6S pre-treatment
LPS
LPS+C6S pre-treatment
IL-6

Figure 6.

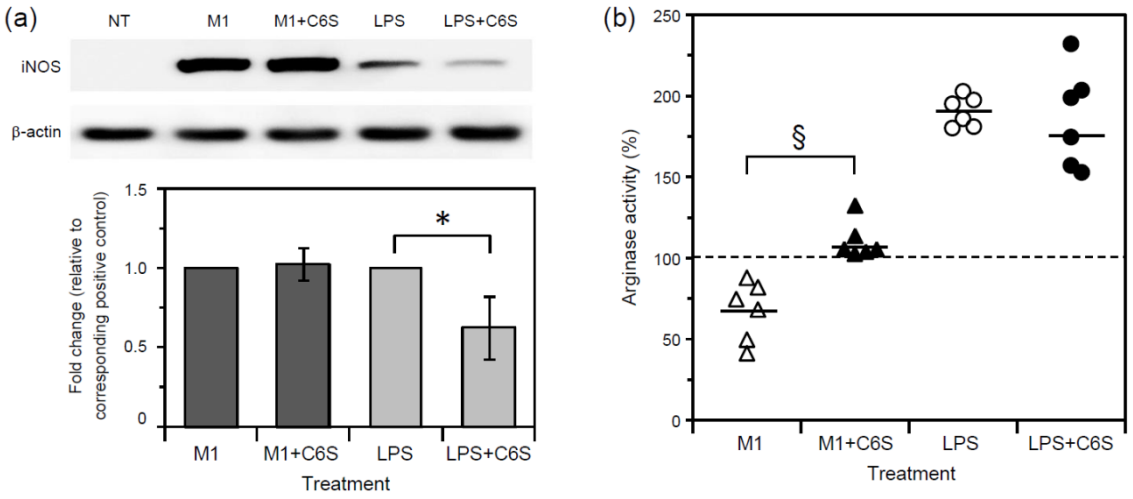
(a)
NT
M1
M1+C6S
LPS
LPS+C6S
iNOS
β-actin
Fold change (relative to corresponding positive control)
1.5
1.0
0.5
0
*
M1
M1+C6S
LPS
LPS+C6S
Treatment
(b)
Arginase activity (%)
250
200
150
100
50
0
§
M1
M1+C6S
LPS
LPS+C6S
Treatment

Figure 7.

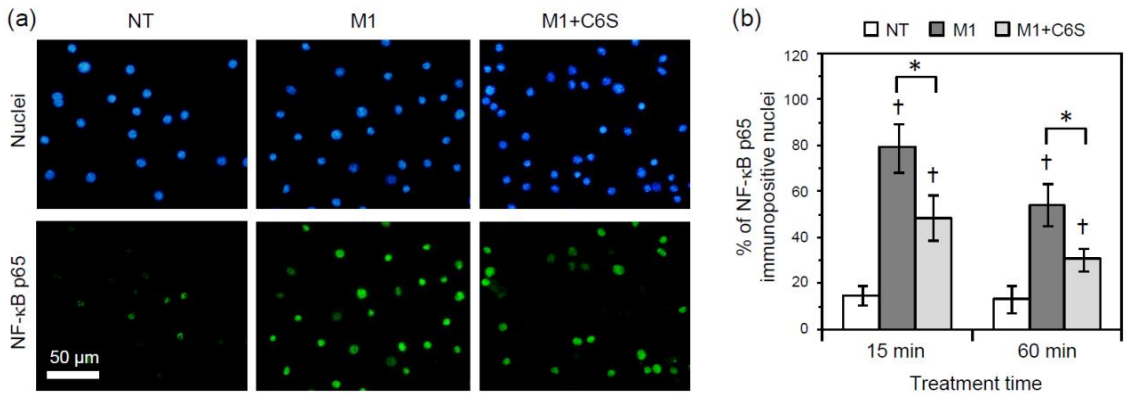
(a)
NT
M1
M1+C6S
Nuclei
NF-κB p65
50 μm
(b)
NT
M1
M1+C6S
% of NF-κB p65 immunopositive nuclei
120
100
80
60
40
20
0
*
*
†
†
†
†
15 min
60 min
Treatment time

Appendix A.

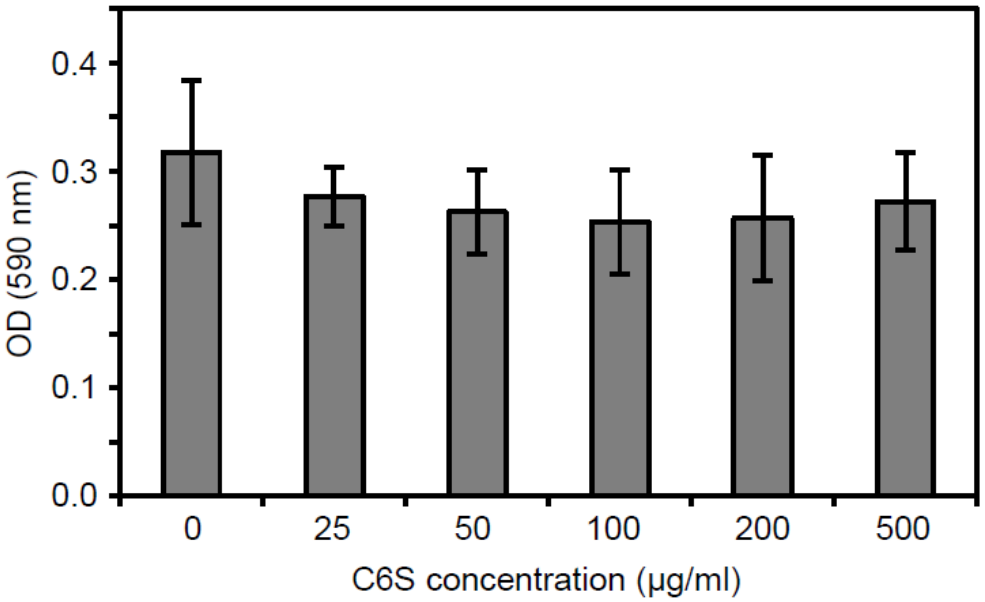
0.4
0.3
0.2
0.1
0.0
OD (590 nm)
0
25
50
100
200
500
C6S concentration (µg/ml)

Appendix B.

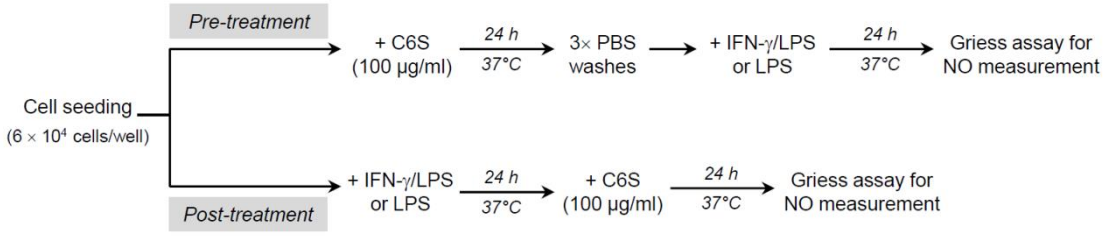
Pre-treatment
+ C6S
(100 µg/ml)
24 h
37°C
3× PBS
washes
+ IFN-γ/LPS
or LPS
24 h
37°C
Griess assay for
NO measurement
Cell seeding
(6 × 10⁴ cells/well)
+ IFN-γ/LPS
or LPS
24 h
37°C
+ C6S
(100 µg/ml)
24 h
37°C
Griess assay for
NO measurement
Post-treatment